Available online at www.sciencedirect.com
ScienceDirect
Journal of Power Sources 173 (2007) 458–466
JOURNAL OF POWER SOURCES
www.elsevier.com/locate/jpowsour

A study of steam methanol reforming in a microreactor

Jeong-Se Suh *, Ming-tsang Lee, Ralph Greif, Costas P. Grigoropoulos

Department of Mechanical Engineering, University of California at Berkeley, Berkeley, CA 94720-1740, USA

Received 20 March 2007; received in revised form 18 April 2007; accepted 18 April 2007
Available online 25 April 2007

Abstract

Steam reforming of methanol is investigated numerically considering both heat and mass transfer of the species in a packed bed microreactor. The numerical results are shown to be in good agreement with experimental data [M.T. Lee, R. Greif, C.P. Grigoropoulos, H.G. Park, F.K. Hsu, J. Power Sources Transport in, 166 (2007) 194–201] with a BASF F3-01($CuO/ZnO/Al_2O_3$) catalyst. A correlation for the conversion efficiency of methanol has been obtained as a function of the operating temperature and a dimensionless time parameter which represents the ratio of the characteristic time of the methanol flow to the time for chemical reaction. The results show that for the constant wall temperature condition the steam reforming process of methanol results in a nearly uniform temperature throughout the microreactor over the range of operating conditions. Published by Elsevier B.V.

Keywords: Fuel cell; Methanol conversion; Steam reforming; Packed-bed reformer; Catalyst

1. Introduction

There is great interest in producing hydrogen for small fuel cell applications to provide high volumetric and gravimetric energy density for miniaturized portable electronic systems [1]. Of special interest is the need to develop efficient microreformers to convert hydrocarbon fuel into hydrogen which can be delivered to a proton exchange membrane fuel cell to produce electricity. Many investigations indicate that methanol is an attractive fuel since it has a high hydrogen-to-carbon ratio relative to gasoline and lower inter-carbon bonds; hence it can be reformed efficiently at moderate temperatures (200–300 °C) [2]. The methanol reformer operating at moderate temperature also produces low CO concentration which is important because of CO contamination of the anode.

Our objective is to examine the conversion efficiency for the production of hydrogen and CO from methanol in a catalyst reforming process. Steam reforming of methanol is achieved by the chemical reaction over a catalyst packed bed at moderate temperature. The steam reforming process of methanol is characterized by the operating temperature, velocity of the steam–methanol mixture reactant, the mass of the catalyst, etc.

Many studies have been carried out to provide insight into the thermal performance and the heat transfer in a steam–methanol reforming reactor. A number of kinetics models for steam–methanol reforming have been reported in the literature [3–8]. Amphlett et al. [3] suggested a semi-empirical kinetics model for the steam–methanol reforming process over the $CuO/ZnO/Al_2O_3$ catalyst, which includes the mathematical model of the reaction rates for the plug flow reactor. Park et al. [9] carried out a one-dimensional analysis for the mass transport in a steam–methanol reformer that employs Amphlett's reaction kinetics model. Karim et al. [10] carried a two-dimensional pseudo-homogeneous analysis for packed bed reactors. In this model, they took the diffusion coefficient of the gas mixture in the reaction process as constant and focused on the effect of heat transfer on the measured methanol conversion. Park et al. [11] carried out a quasi three-dimensional analysis of the reacting flow in a steam–methanol reformer, coupled to three-dimensional heat transfer in a silicon wafer. Yuan et al. [12] simulated in a three-dimensional study the heat and mass transport in a methane–steam reforming duct considering the catalytic chemical reactions.

* Corresponding author. Permanent address: Department of Mechanical Engineering, ReCAPT, Gyeongsang National University, Jinju 660-701, Korea. Tel.: +82 55 751 5312; fax: +82 55 751 5622.
E-mail address: jssuh@gnu.ac.kr (J.-S. Suh).

0378-7753/$ – see front matter. Published by Elsevier B.V.
doi:10.1016/j.jpowsour.2007.04.038

Nomenclature

a_p	Porous surface area per unit volume of pellet [$m^2\ m^{-3}$]
A_b	Cross-sectional area of bed [m^2]
A, B	Pre-exponential term in the Arrhenius expression for k
c_1	Concentration of methanol [$mol\ m^{-3}$]
$c_{p,i}$	Specific heat of species i [$J\ kg^{-1}\ K$]
C_D, C_R	Modification factors of decomposition and reforming reaction
d_p	Diameter of catalyst pellet [m]
D_h	Characteristic diffusion length [m]
$D_{1,eff}$	Effective diffusivity [$m^2\ s^{-1}$]
D_{1m}	Ordinary diffusivity [$m^2\ s^{-1}$]
D_{Kl}	Knudsen diffusivity [$m^2\ s^{-1}$]
E	Activation energy in the Arrhenius expression for k [$J\ mol^{-1}$]
F_l	Feed rate of liquid mixture [$m^3\ s^{-1}$]
k_i	Thermal conductivity of species i [$W\ m^{-1}\ K$]
k_D'''	Volumetric reaction constant for decomposition [$mol\ kg\ s^{-1}$]
$\bar{k}_D'''$	Modified reaction constant for decomposition, $(1-\varepsilon)\rho_s k_D'''$ [$mol\ m^{-3}\ s$]
k_R''	Surface reaction constant [$m\ s^{-1}$]
k_R'''	Volumetric reaction constant for reforming [$m^3\ kg^{-1}\ s$]
$\bar{k}_{R,0}'''$	Modified reaction constant for reforming at $T=220\,^\circ C$, $(1-\varepsilon)\rho_s k_R'''$ [s^{-1}]
ΔH	Enthalpy of reaction [$J\ mol^{-1}$]
L_b	Length of bed [m]
Le	Lewis number, $Le=\rho_g c_{p,g} D_{1m}/k_g$
m_i	Mass fraction of species i
m_s	Mass of catalyst [kg]
m'''	Volumetric mass source [$kg\ m^{-3}\ s$]
$\bar{m}_{CO}$	Cross sectional area-weighted average of CO mass concentration [ppm]
M_i	Molecular weight of species i [$kg\ mol^{-1}$]
P	Pressure [Pa]
q'''	Volumetric heat source [$W\ m^{-3}$]
r, z	Radial and axial Cartesian coordinates [m]
r_i'''	Volumetric chemical reaction rate of species i [$mol\ m^{-3}\ s$]
r_{pore}	Pore size of pellet [m]
$\bar{R}$	Universal gas constant [$J\ mol^{-1}\ K$]
Re	Reynolds number
S	Surface area [m^2]
Sc	Schmidt number
Sh	Sherwood number
SMR	Molar ratio of steam to methanol
S_p	Pellet surface [m^2]
T	Temperature [K, °C]
U	Velocity of mixture [$m\ s^{-1}$]
V	Volume [m^3]
x_i	Mole fraction of species i
$\bar{x}_i$	Cross sectional area-weighted average of mole fraction of species i

Greek symbols

ε	Porosity
η	Conversion efficiency
μ	Dynamic viscosity [Pa s]
ν	Viscosity [$m^2\ s^{-1}$]
ρ	Density [$m^3\ kg^{-1}$]
σ, Ω	Lennard Jones Parameters
τ	Tortuosity factor

Subscripts

0	Inlet, reference
b	Bed
D	Decomposition
g	Gas mixture
i	Species
l	Liquid
m	Average
p	Pellet
R	Reforming
s	Solid

In this work, we have analyzed the methanol–steam reformer considering the two-dimensional variation of the transport and thermal properties of the gas mixture associated with the composition of each species throughout the reformer. The effect of wall temperature on the conversion efficiency and CO production from methanol in the reformer has been investigated with the feed rate of the water–methanol mixture and the mass of the catalyst as parameters. For the commercial BASF F3-01($CuO/ZnO/Al_2O_3$) catalyst, a correlation for the conversion efficiency of methanol has been presented as a function of the wall temperature of the reformer and a dimensionless time parameter that is related to the flow rate of the steam–water mixture fed to the reactor, the catalyst mass and the reaction rate. In addition, the numerical results for the conversion efficiency of methanol and the amount of CO produced in the reformer have been compared with experimental data [13] and with a one-dimensional analytical solution [9].

2. Analysis of steam methanol reforming process

2.1. Chemical kinetics of catalyst steam methanol reforming

Methanol can be reformed by two overall reactions in a reformer filled with the catalyst $CuO/ZnO/Al_2O_3$ as described by Amphlett et al. [3]:

$$CH_3OH + H_2O \xleftrightarrow{k_R} CO_2 + 3H_2 \quad (1)$$

$$CH_3OH \xleftrightarrow{k_D} CO + 2H_2 \quad (2)$$

where the subscript 'R' refers to steam reforming, and 'D' refers to decomposition. Methanol is primarily reformed via reaction (1) called reforming. Some portion of the methanol also decomposes directly to CO via reaction (2). In addition, the water–gas shift reaction adjusts the composition of the product gas:

$$CO + H_2O \leftrightarrow CO_2 + H_2 \tag{3}$$

The water–gas shift reaction [reaction (3)] can be neglected without a substantial loss in accuracy of methanol concentrations as described by Amphlett et al.[3]. For a packed bed, the chemical reaction rates can be expressed in terms of reaction rate constants and the concentration of methanol according to

$$r_R''' = (1-\varepsilon)\,\rho_s k_R''' c_1, \qquad r_D''' = (1-\varepsilon)\,\rho_s k_D''' \tag{4}$$

where ρ_s is the solid density of the catalyst, and k_R''' and k_D''' are the rate constants for reforming and decomposition, respectively. The reaction rate constants depend on the properties of the catalyst surface and on the temperature. These quantities can be related to the rate constants of Amphlett et al. [3] which are derived from an Arrhenius relation as follows:

$$k_R''' = C_R(A_R + B_R \ln \mathrm{SMR})\, e^{(-E_R/\bar{R}T)} \tag{5}$$

$$k_D''' = C_D A_D e^{(-E_D/\bar{R}T)} \tag{6}$$

where SMR is the molar ratio of steam to methanol; A_R, B_R, and A_D are Amphlett's constants ([3]) for reforming and decomposition reactions, respectively. C_R and C_D are correction factors for reforming and decomposition reactions, respectively, and can be determined empirically from the activity and effectiveness of catalyst. From the experimental data [13] for BASF F3-01($CuO/ZnO/Al_2O_3$) catalyst, the correction factors are determined to have the values of 5.5 in the reforming reaction and 3.5 in the decomposition reaction, respectively. The generation rates of the species can be expressed as

$$r_1''' = -r_R''' - r_D''' \tag{7a}$$

$$r_2''' = -r_R''' \tag{7b}$$

$$r_3''' = r_R''' \tag{7c}$$

$$r_4''' = r_D''' \tag{7d}$$

$$r_5''' = 3r_R''' + 2r_D'''. \tag{7e}$$

where the subscripts are 1 = CH_3OH, 2 = H_2O, 3 = CO_2, 4 = CO, and 5 = H_2.

2.2. Heterogeneous catalytic reaction rate

The methanol reforming reaction occurs on the catalyst particles in a packed bed during the reforming of a steam–methanol mixture. It also includes the heat and mass transfer in the catalyst porous medium of the packed bed. The mass transport considerations control the rate of reaction, while heat transfer considerations control the rate at which the heat of reaction can be removed, and hence the temperature of the reaction. Our analysis for reaction rate is undertaken by considering the mass diffusion of methanol from the free stream to the surface of the catalyst pellet, and into the pores of the pellet. The heterogeneous reaction rate within the packed bed of catalyst r_R''' can be expressed by [14,15]

$$r_R''' = (1-\varepsilon)\frac{S_p r_R''}{V_p} \tag{8}$$

where S_p is the surface of pellet within the packed bed of catalyst, V_p is the volume of the pellet, and r_R'' is the molar flux of methanol at the surface of pellet. The methanol–steam mixture diffuses into the pores of the pellet and encounters two resistances; one is a convective resistance between the free stream and pellet surface, and the other is a diffusive resistance within the pellet pore. The molar flux r_R'' depends on both the concentration of the methanol at the surface of pellet and the two resistances [16]

$$r_R'' = \frac{c_1}{\frac{1}{(V_p a_p/S_p)\,\eta_p k_R''} + \frac{D_h}{\mathrm{Sh} D_{1m}}} \tag{9}$$

where c_1 is the concentration of methanol in the free stream between the pellets, a_p is the porous surface area per unit volume of pellet, D_h is the characteristic diffusion length in the packed bed defined by $D_h = \varepsilon d_p/(1-\varepsilon)$, η_p is the effectiveness of catalyst pellet, and k_R'' is the first order kinetic rate constant for the reaction. The kinetic rate constant k_R'' in Eq. (9) is defined per unit the surface area of pellet and related to the reaction rate constant k_R''' in Eq. (5), $k_R'' = k_R''' \rho_s / a_p$. The effectiveness of the catalyst pellet is the ratio of the actual reaction rate divided by that for a pellet with an infinite diffusion coefficient and can be taken for a spherical pellet to be [16]

$$\eta_p = \frac{1}{\Lambda}\left(\frac{1}{\tanh 3\Lambda} - \frac{1}{3\Lambda}\right), \qquad \Lambda = \frac{V_p}{S_p}\sqrt{\frac{k_R'' a_p}{D_{1,\mathrm{eff}}}} \tag{10}$$

where $D_{1,\mathrm{eff}}$ is the effective diffusivity within the catalyst pellet and includes ordinary diffusion (D_{1m}) and Knudsen diffusion (D_{K1}) [16]:

$$\frac{1}{D_{1,\mathrm{eff}}} = \frac{\tau_p}{\varepsilon_p}\left(\frac{1}{D_{1m}} + \frac{1}{D_{K1}}\right) \tag{11}$$

$$D_{1m} = \frac{1-x_1}{\sum_{i=2}^{5}(x_i/D_{1i})},$$

$$D_{1i} = 1.86\times 10^{-7}\frac{\sqrt{T^3\left(\frac{1}{M_1}+\frac{1}{M_i}\right)}}{\sigma_{1i}^2 \Omega_D P} \tag{12}$$

$$D_{K1} = \frac{2}{3} r_{\mathrm{pore}}\sqrt{\frac{8\bar{R}T}{\pi M_1}}. \tag{13}$$

The correlation for a dry packed bed for the Sherwood number (Sh), defined as a dimensionless mass transfer conductance in Eq. (9), depends on Reynolds number (Re) and Schmidt number

(*Sc*) as follows[17]:

$$Sh = (0.5\,Re0.5 + 0.2\,Re2/3)Sc^{1/3},$$

$$Re = \frac{\rho_g U D_h}{\mu_g}, \quad Sc = \frac{\nu_g}{D_{1m}}. \tag{14}$$

where the density of the gas mixture ρ_g is the mass-weighted average of the density of species assuming an ideal gas mixture and can be expressed as follows:

$$\rho_g = \frac{P}{\bar{R}T} M = \frac{P}{\bar{R}T} \sum_{i=1}^{5} x_i M_i. \tag{15}$$

The viscosity of the gas mixture μ_g in Eq. (14) can be calculated from Wilke's mixture rule [18] as follows:

$$\mu_g = \sum_{i=1}^{5} \frac{x_i \mu_i}{\sum_{j=1}^{5} x_j X_{ij}} \tag{16}$$

$$X_{ij} = \frac{[1 + (\mu_i/\mu_j)^{1/2}(M_j/M_i)^{1/4}]^2}{\sqrt{8}\,[1 + (M_i/M_j)]^{1/2}} \tag{17}$$

2.3. Conservation equations

The methanol–steam reformer configuration is axisymmetric as shown in Fig. 1, and includes the isotropic and continuously distributed catalyst. The flow of the steam–methanol mixture is assumed to be steady and radially uniform through the inert catalyst packed bed. The mixture consists of five species, taken to be ideal gases, and reacts heterogeneously with the catalyst. It is also assumed that the thermal state of the catalyst and the gas mixture is locally in equilibrium and the Lewis numbers of all species are equal to unity, $\mathrm{Le} = \rho_g c_{p,g} D_{1m}/k_g = 1$. The Cartesian cylindrical coordinate system is used with the z-axis coincident with the apex of the flow region as shown in Fig. 1. The mass conservation of the gas mixture can be expressed as

$$\frac{\mathrm{d}}{\mathrm{d}z}(\varepsilon \rho_g U) = 0, \tag{18}$$

where U is the mean velocity of the gas mixture, and ε is the catalyst porosity given by $\varepsilon = 1 - (V_s/V)$. The equation for the conservation of energy reduces to [19]

$$\varepsilon \rho_g c_{p,g} U \frac{\partial T}{\partial z} = \frac{1}{r}\frac{\partial}{\partial r}\left(r k_m \frac{\partial T}{\partial r}\right) + \frac{\partial}{\partial z}\left(k_m \frac{\partial T}{\partial z}\right) + q'''_m, \tag{19}$$

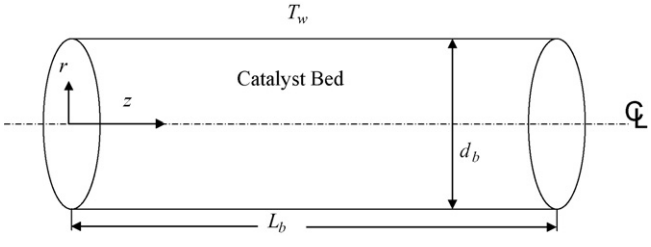

Fig. 1. Schematic of the modeling domain in the reactor.

where k_m is a volume-weighted average conductivity of the catalyst material and gas mixture, and q'''_m is the volumetric heat source of the porous medium generated from the heterogeneous reaction between the gas mixture and catalyst:

$$k_m = (1 - \varepsilon)\,k_s + \varepsilon k_g. \tag{20}$$

$$q'''_m = -\Delta H_R r'''_R - \Delta H_D r'''_D. \tag{21}$$

The specific heat of the gas mixture $c_{p,g}$ is obtained from the mass-weighted average for each species, $c_{p,g} = \sum_{i=1}^{5} m_i c_{p,i}$ [16]. The thermal conductivity of the gas mixture k_g is calculated in the same manner as μ_g (cf. Eqs. (16) and (17)) from Wilke's mixture rule [18]. The conservation of mass equation for species i reduces to [19]

$$\varepsilon \rho_g U \frac{\partial m_i}{\partial z} = \frac{1}{r}\frac{\partial}{\partial r}\left(r \rho_g D_m \frac{\partial m_i}{\partial r}\right) + \frac{\partial}{\partial z}\left(\rho_g D_m \frac{\partial m_i}{\partial z}\right) + m'''_{g,i} \tag{22}$$

where m_i is the mass fraction of gas component i defined by $m_i = \rho_i/\rho_g$, D_m is the mean diffusivity of the gas mixture in the porous media, and $m'''_{g,i}$ is the mass generation of gas component i:

$$D_m = \varepsilon D_{1m}. \tag{23}$$

$$m'''_{g,i} = M_i r'''_i \tag{24}$$

A constant tube wall temperature, $T = T_w$, is specified. The temperature of the gas mixture at the inlet is taken to be the same as that of the wall. The mass transfer for each of the species is impermeable through the tube wall, $\partial m_i/\partial r|_{r=d_b/2} = 0$. The liquid mixture of water and methanol is considered to have been preheated and then flows as a gas mixture into the packed catalyst at $z = 0$. The molar ratio of water to methanol is prescribed and the velocity of the gas mixture is uniform. The physical parameters and basic operating conditions are listed in Table 1 and the other physical gas properties of each species are referred to the existing literatures [16,20–22].

2.4. Numerical procedure

The governing equations were solved numerically using the method of Karki and Patankar [23]. The governing equations

Table 1
Geometric parameters and physical properties

Diameter of catalyst bed (d_b)	1.0×10^{-3} m
Axial length of catalyst bed (L_b)	10×10^{-3} m
Diameter of pellet (d_p)	150×10^{-6} m
Porous surface area of pellet (a_p)	1.92×10^{8} m^2 m^{-3}
Pore size of pellet (r_{pore})	1.0×10^{-7} m
Porosity of catalyst bed (ε)	0.35
Density of catalyst (ρ_s)	1300 kg m^{-3}
Thermal conductivity of catalyst (k_s)	20 W m^{-1} K (Touloukian [22])
Void–tortuosity ratio factor (ε_p/τ_p)	0.2 (Mills [16])
Lennard Jones parameter (σ_{1i})	(Mills [16] A.26)
Lennard Jones parameter (Ω_D)	(Mills [16] A.28)
Molar ratio of steam to methanol (SMR)	1.1

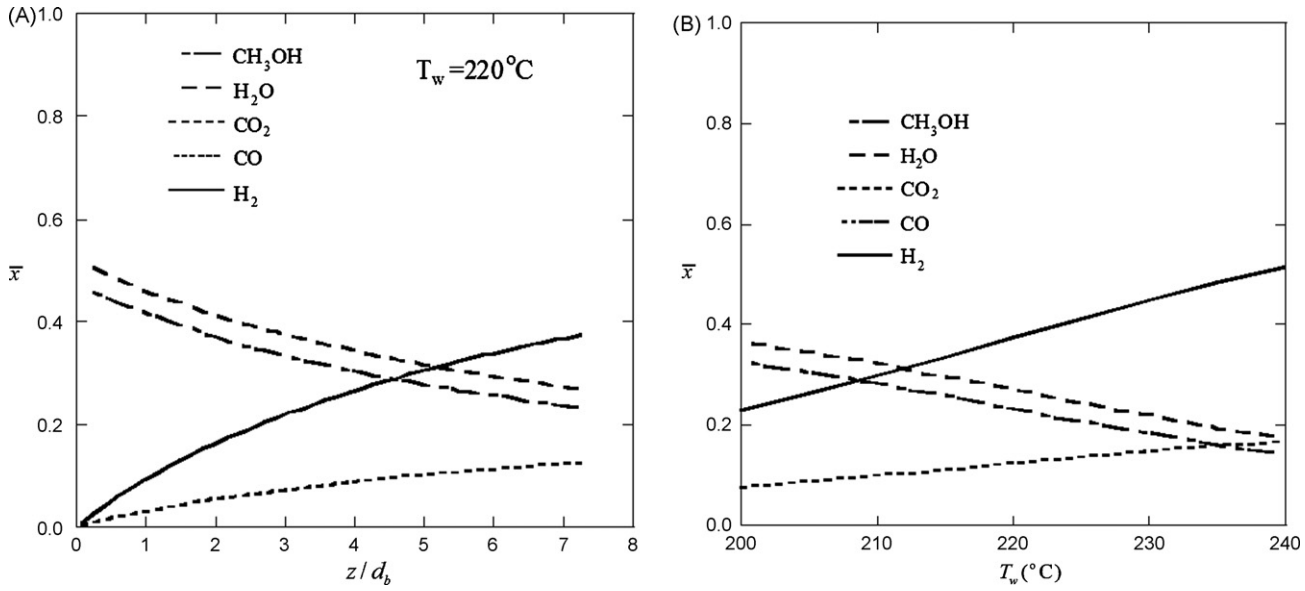

Fig. 2. Molar fraction variations of the components for the feed water–methanol flow rate of 10 μl min^{-1}: (A) molar fraction variations of species along the axial direction of the reactor and (B) molar fraction variations of species with respect to T_w leaving the reactor.

are transformed into the curvilinear cylindrical coordinate system $r = r(\xi, \eta)$ and $z = z(\xi,\eta)$ and the equations are discretized using the central difference scheme [24]. The resulting algebraic equations were solved using a nonuniform grid system with 71 nodes in the ξ direction and 45 nodes in the η direction. In the region near the surface and in the vicinity of the tube wall, the grids were densely distributed. Iterations were continued until changes in the mass fractions were less than 0.1%. It was found that the results for the temperatures and mass fractions are differed by less than 0.01% from a grid system of 90 × 142 nodes.

3. Results and discussion

In this work, results are obtained for a methanol steam reformer for a circular tube packed with the BASF F3-01($CuO/ZnO/Al_2O_3$) catalyst, and investigated over the following range of conditions: 200 °C ≤ T_w ≤ 240 °C, 5 mg ≤ m_s ≤ 25 mg, 5 μl/min ≤ $F_{l,0}$ ≤ 25 μl min^{-1}, 0.5 mm ≤ d_b ≤ 4 mm, 2 mm ≤ L_b ≤ 20 mm.

Fig. 2 shows the molar fraction variations of the components produced for the feed water–methanol flow rate of 10 μl min^{-1}. As shown in Fig. 2(A), when the steam–methanol mixture decomposes at the constant wall temperature, T_w = 220 °C, the main components produced are hydrogen and CO_2, and only a small amount of CO is produced, which is not discernible in the figure. As the steam–methanol mixture is gradually reformed throughout the reactor, the molar fractions of hydrogen and CO_2 increase along the axial length of the reactor. Fig. 2(B) shows nearly linear variations of the mole fractions of each species leaving the reactor as a function of the wall temperature. The increase of H_2 produced, as shown in Fig. 2(B), in the reformer is attributed to the activation of the chemical reaction of methanol with respect to an increase of the operating temperature.

The conversion efficiency of methanol as a function of the wall temperature is shown in Fig. 3 for three values of the catalyst mass for a feed water-methanol flow rate of 10 μl min^{-1}. The effect of increasing wall temperature is to almost linearly increase the conversion efficiency of methanol in the reformer. The methanol conversion rate increases with increasing catalyst mass.

The influence of the catalyst mass on the flow rate of the products leaving the reactor is shown in Fig. 4 for the mixture feed flow rate of 10 μl min^{-1}. The molar flow rates of H_2 and CO_2 increase with increasing catalyst mass. The flow rate of CO also increases with the catalyst mass, but is not discernible in the figure.

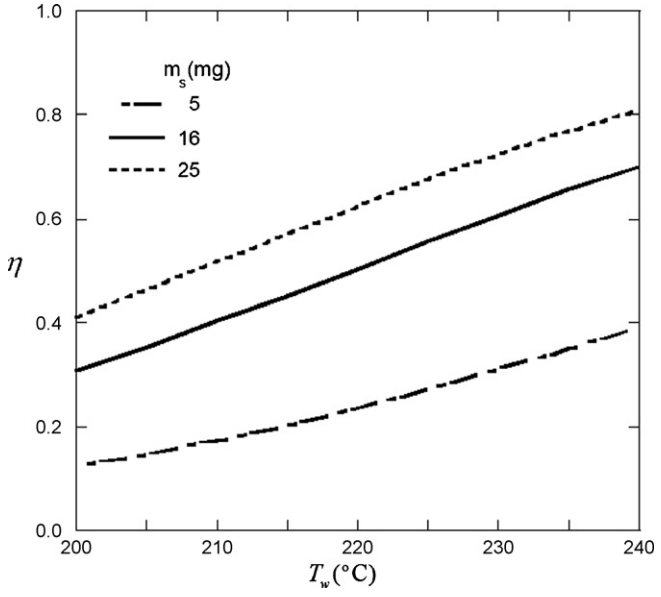

Fig. 3. Conversion efficiency of methanol for three cases of catalyst mass for the feed water-methanol flow rate of 10 μl min^{-1}.

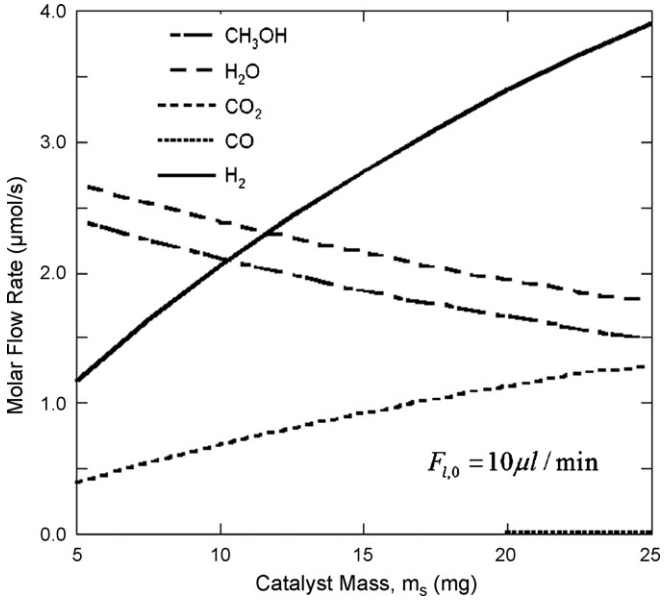

Fig. 4. Influence of the catalyst mass on the flow rate of species leaving the reactor for a feed water–methanol flow rate of 10 μl min^{-1}.

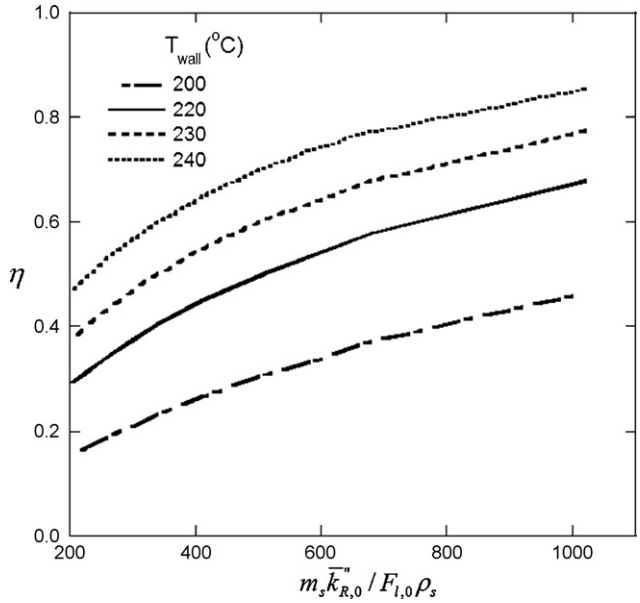

Fig. 6. Results for the conversion efficiency of methanol as a function of the dimensionless parameter.

The conversion efficiency of methanol for three values of the feed flow rate of the mixture is shown in Fig. 5 as a function of the wall temperature. The conversion efficiency of methanol decreases with increasing feed flow rate. This is because the mixture stays in the catalyst packed bed for a shorter time with increasing flow rate, which results in less reaction with the catalyst.

Peppley et al. [4] refer to a fractional methanol conversion as a function of a parameter related to the ratio of the catalyst mass to the feed flow rate of the mixture, $m_s/F_{l,0}$. This parameter can be modified into a dimensionless parameter, $m_s\bar{k}'''_{R,0}/F_{l,0}\rho_s$.

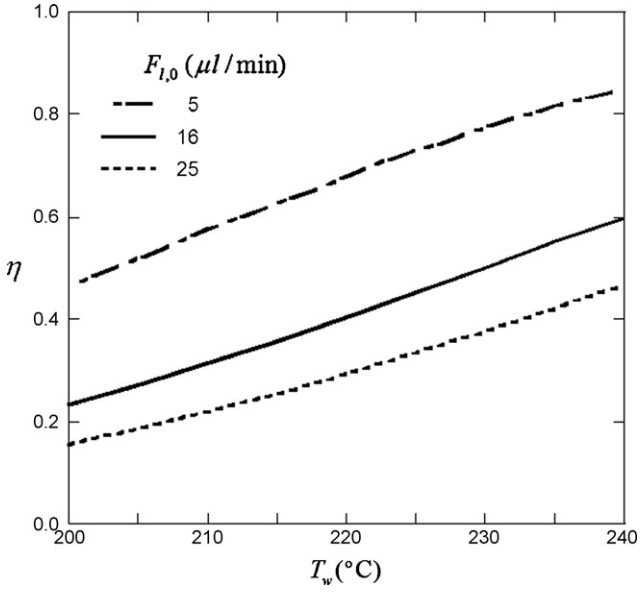

Fig. 5. Conversion efficiency of methanol for three cases of feed flow rate for $m_s = 16$ mg.

Considering the relations $m_s = \rho_s A_b L_b$ and $F_{l,0} = U_l A_b$, this parameter is related to the parameter, $L_b\bar{k'''}_{R,0}/U$(cf. Eq. (27) discussed below, where $\bar{k}'''_{R,0} = (1-\varepsilon)\,\rho_s k'''_{R,0}$). This dimensionless parameter is related to the ratio of the characteristic time of the methanol flow, $m_s/F_{l,0}\rho_s$ to the time for the methanol chemical reaction in the reformer, $1/\bar{k}'''_{R,0}$. Results for the conversion efficiency of methanol are shown for four wall temperatures in Fig. 6 in terms of the dimensionless time parameter, $m_s\bar{k}'''_{R,0}/F_{l,0}\rho_s$. The conversion efficiency of methanol increases for increasing values of $m_s\bar{k}'''_{R,0}/F_{l,0}\rho_s$. Based on the numerical results, the conversion efficiency of methanol is correlated as follows:

$$\eta = -1.222 + 0.00061T\,(K) - (1.087 - 0.0033T\,(K))\ln\left(\frac{m_s\bar{k}'''_{R,0}}{F_{l,0}\rho_s}\right) \quad (25)$$

This correlation agrees with the calculated conversion efficiency with an error less than 0.1% over the range of operating conditions.

The numerical results for the conversion efficiency of methanol are now compared with both experimental data [13] and the results from a one-dimensional analysis. Considering the molar ratio of steam to methanol, SMR, the one-dimensional analytical solution for the conversion rate of methanol is given by [9,13]:

$$\eta \equiv \frac{\bar{x}_{CH_3OH,0} - \bar{x}_{CH_3OH}}{\bar{x}_{CH_3OH,0}} = \frac{\xi\,(SMR+3)}{2\,\xi + SMR + 1} \quad (26)$$

where ξ is

$$2\,\xi + (SMR+3)\ln(1-\xi) = -\frac{L_b}{U/[\bar{k'''}_R(SMR+1)]} \quad (27)$$

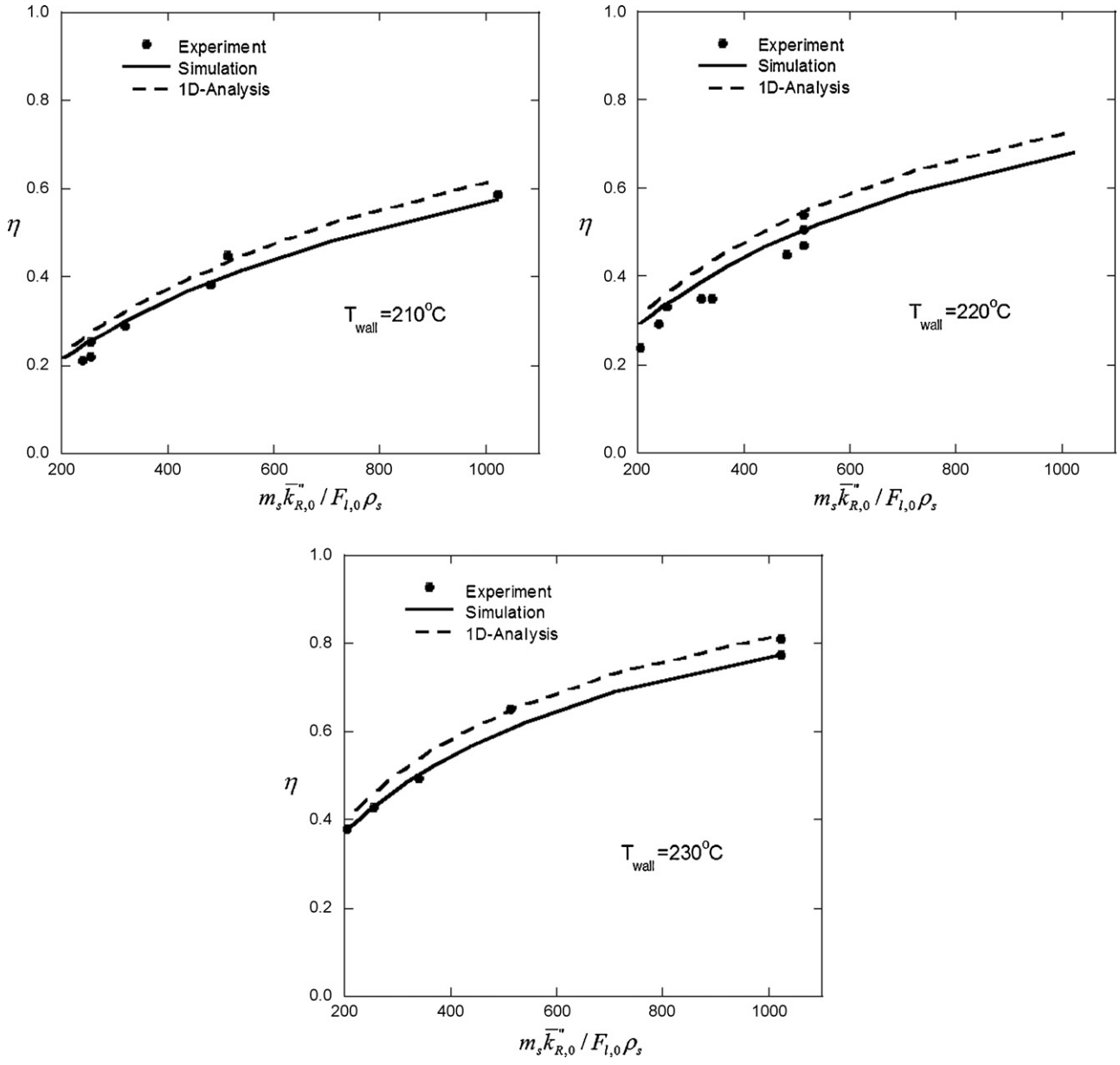

Fig. 7. Comparison of the numerical results for the conversion efficiency of methanol with the experimental and analytical results for three wall temperatures: (A) $T_w = 210\,^{\circ}C$, (B) $T_w = 220\,^{\circ}C$, and (C) $T_w = 230\,^{\circ}$.

The numerical results for the conversion efficiency of methanol, along with the experimental and one-dimensional analytical results, are shown in Fig. 7 as a function of the dimensionless parameter $m_s\bar{k}'''_{R,0}/F_{l,0}\rho_s$ for three wall temperatures. There is general agreement among all of the results; the numerical results are slightly lower than the one-dimensional results.

An accurate determination of the CO produced from reaction (2) is important because CO deactivates the Pt catalyzed anode of fuel cells. The analytical solution for the mass fraction of CO produced in the catalyst can be obtained from [9] as follows:

$$\bar{m}_{CO} = \frac{\bar{k}'''_D}{\rho_g U} M_{CO} L_b \times 10^6 \tag{28}$$

where $\bar{m}_{CO}$ is the mass concentration of CO (ppm) leaving the reactor, $\bar{k}'''_D$ is the rate constant of decomposition reaction defined by $(1-\varepsilon)\,\rho_s k'''_D$, and M_{CO} is the molecular weight of CO. Fig. 8 shows the results for the mass fraction of CO leaving the reactor for three wall temperatures. The numerical and the analytical results are in fairly good agreement with one another but they differ significantly from the experimental data [13]. At the highest wall temperature (230 °C), the predictions are much greater than the experimental data.

It is also noted that for the conditions studied, the numerical results yield little variation for the molar fraction of each species in the radial direction. In addition, for the constant wall temperature condition of this study, there is little variation of the gas temperature in both the radial and axial directions.

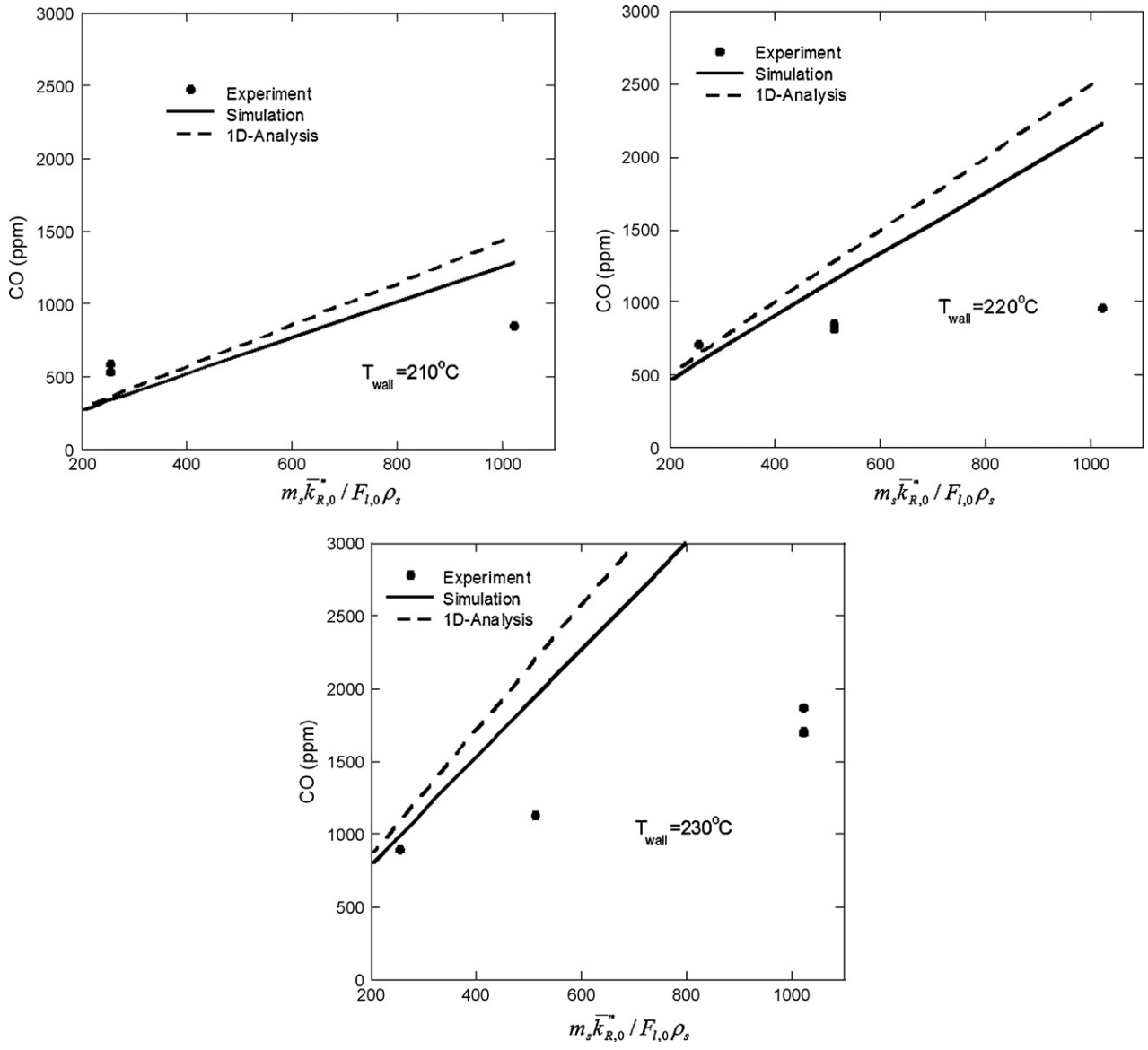

Fig. 8. Comparison of numerical results for the mass fraction of CO leaving the reactor with experimental and analytical results in three cases of wall temperature: (A) $T_w = 210\,^{\circ}C$, (B) $T_w = 220\,^{\circ}C$, and (C) $T_w = 230\,^{\circ}C$.

4. Conclusions

The conversion characteristics of the steam reforming of methanol in a microreactor tube packed with a commercial BASF F3-01($CuO/ZnO/Al_2O_3$) catalyst have been investigated by numerical simulation, considering both the heat and mass transfer of the species. The numerical results for the conversion efficiency of methanol agree with a one-dimensional analytical solution [9] and with experimental data [13] over the range of operating conditions. From the numerical results, a correlation for the conversion efficiency of methanol over the range of operating conditions is presented as a function of the operating temperature and a dimensionless time parameter which represents the ratio of the characteristic time of the methanol flow to the time for the chemical reaction of methanol. For the mass fraction of CO leaving the reactor, the numerical and one-dimensional analytical results are in fairly good agreement, but they differ significantly from experimental data. At the highest wall temperature (230 °C), the numerical and analytical results are much greater than the experimental data. The numerical results yield little variation for the molar fraction of each species in the radial direction. In addition, there is little variation of the gas temperature in both the radial and axial directions for the constant wall temperature condition of this study.

Acknowledgements

We thank Stephen Sharratt and Allan Chen of the University of California at Berkeley who assisted in carrying out the measurements. This work was partially supported by the Industrial Technology and Research Institute (ITRI) in Taiwan, R.O.C., and the Berkeley ITRI Research Center (BIRC). Professor J.-S. Suh wishes to acknowledge support from the 2nd BK and the NURI Projects of Gyeongsang National University in Korea.

References

[1] A.F. Ghenciu, Curr. Opin. Solid State Mater. Sci. 6 (2002) 389–399.
[2] L.F. Brown, Int. J. Hydrogen Energy 26 (2001) 381–397.
[3] J.C. Amphlett, K.A.M. Creber, J.M. Davis, R.F. Mann, B.A. Peppley, D.M. Stokes, Int. J. Hydrogen Energy 19 (1994) 131–137.
[4] B.A. Peppley, J.C. Amphlett, L.M. Kearns, R.F. Mann, Appl. Catal. 179 (1999) 21–29.
[5] B.A. Peppley, J.C. Amphlett, L.M. Kearns, R.F. Mann, Appl. Catal. A-Gen. 179 (1999) 31–49.
[6] J. Agrell, H. Birgersson, M. Boutonnet, J. Power Sources 106 (2002) 249–257.
[7] J.K. Lee, J.B. Ko, D.H. Kim, Appl. Catal. A-Gen. 278 (2004) 25–35.
[8] Y.T. Choi, H.G. Stenger, J. Power Sources 142 (2005) 81–91.
[9] H.G. Park, M.T. Lee, F.K. Hsu, C.P. Grigoropoulos, R. Greif, Proc. IMECE 2004 (2004) 1–7.
[10] A. Karim, J. Bravo, A. Datye, Appl. Catal. A: Gen. 282 (2005) 101–109.
[11] H.G. Park, J.A. Malen, W.T. Piggott, J.D. Morse, R. Greif, C.P. Grigoropoulos, M.A. Havstad, R. Upadhye, J. Microelectromech. Syst. 15 (2006) 976–985.
[12] J. Yuan, F. Ren, B. Sunden, Int. J. Heat Mass Transfer 50 (2007) 687–701.
[13] M.T. Lee, R. Greif, C.P. Grigoropoulos, H.G. Park, F.K. Hsu, J. Power Sources 166 (2007) 194–201.
[14] L.D. Schmidt, The Engineering of Chemical Reactions, Oxford University Press, New York, 2005.
[15] C.G. Hill, An Introduction to Chemical Engineering Kinetics and Reactor Design, John Wiley and Sons, 1977.
[16] A.F. Mills, Mass Transfer, Prentice Hall, Upper Saddle River, N.J., 2001.
[17] A.F. Mills, Heat Transfer, Prentice Hall, Upper Saddle River, N.J., 1999.
[18] C.R. Wilke, J. Chem. Phys. 18 (1950) 517–519.
[19] D.A. Nield, A. Bejan, Convection in Porous Media, Springer Science-Business Media, New York, 2006.
[20] N.B. Vargaftik, Tables of Thermophysical Properties of Liquids and Gases, McGraw-Hill, New York, 1975.
[21] F.P. Incropera, D.P. Dewitt, Fundamentals of Heat and Mass Transfer, John Wiley and Sons, 2002.
[22] Y.S. Touloukian, Thermal Conductivity: Nonmetallic Solids, IFI/Plenum, New York, 1970.
[23] K.C. Karki, S.V. Patankar, Numerical Heat Transfer 14 (1988) 295–307.
[24] S.V. Patankar, Numerical Heat Transfer and Fluid Flow, Hemisphere, Washington, DC, 1980.